Environmental Science & Technology

Article

pubs.acs.org/est

Interactions between Algal Extracellular Polymeric Substances and Commercial TiO_2 Nanoparticles in Aqueous Media

Adeyemi S. Adeleye*,† and Arturo A. Keller*

Bren School of Environmental Science & Management, and University of California Center for Environmental Implications of Nanotechnology, University of California, Santa Barbara, California 93106-5131, United States

Supporting Information

ABSTRACT: The implications of engineered nanomaterials (ENMs) in the environment are often investigated using pristine particles. However, there are several biogenic and geogenic materials in natural waters that interact with and modify the surface of ENMs, thereby influencing their fate and effects. Here we studied the influence of soluble extracellular polymeric substances (sEPS) produced by freshwater and marine algae on the surface properties and fate of three commercial TiO_2 nanoparticles ($nTiO_2$) with different coatings. Adsorption of sEPS by the various $nTiO_2$ is dependent on particle surface area, intrinsic $nTiO_2$ surface charge, and hydrophobicity. Interactions between sEPS and $nTiO_2$ were driven by electrostatic interactions and chemical bonding (bridge-coordination) between the COO^- group of sEPS and $nTiO_2$. Charge reversal of positively charged $nTiO_2$ was observed at pH 7 in the presence of 0.5 mg-C/L sEPS. In addition, the critical coagulation concentration (CCC) of $nTiO_2$ increased in the presence of sEPS—from both freshwater and marine sources. CCC of all nTiO2 increased as sEPS concentrations increased. This study shows that naturally occurring sEPS can modify the surface properties and fate of $nTiO_2$ in natural waters, and should be accounted for when predicting the fate and effects of engineered nanomaterials in the environment.

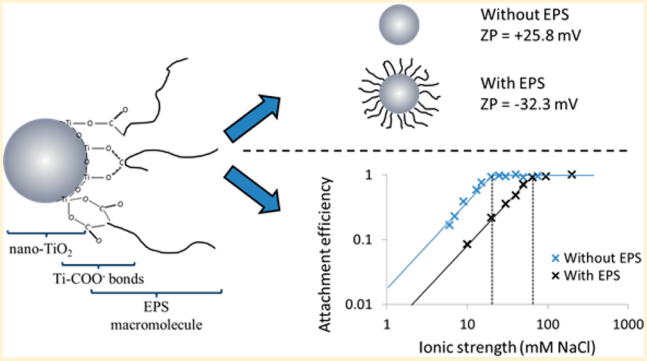

1.0. INTRODUCTION

Nanosized titanium dioxide ($nTiO_2$) is one of the most-manufactured and used engineered nanomaterials (ENMs).[1] Common uses of $nTiO_2$—such as in personal care products, paints and coatings, and cleaning products, etc.—will likely lead to direct release of the ENMs into the environment.[2] A thorough understanding of the fate of $nTiO_2$ in aquatic systems is necessary for a reliable environmental risk assessment of these particles in natural waters. Most previous studies have considered pristine, uncoated $nTiO_2$,[3−5] while in fact almost all commercially available $nTiO_2$ is coated for different applications.

The fate and effect of ENMs in natural waters depend on the physicochemical properties of particles as well as their interactions with other factors present in media.[6,7] Homoaggregation, and more importantly, heteroaggregation between ENMs and other naturally occurring colloids determine ENM fate in aquatic systems.[6−8] Natural organic matter (NOM) also affects the stability of ENMs via direct interactions as well as influencing heteroaggregation of $nTiO_2$ with natural colloids.[6] The effect of commonly used proxies of NOM such as humic acid, fulvic acid, alginate, etc. on the stability of $nTiO_2$ is well understood.[3,4,9] The influence of a different type of NOM solely produced by microorganisms, known as extracellular polymeric substances (EPS), on the stability of $nTiO_2$ in aquatic systems is however largely uninvestigated.

About 50% of phytoplankton photosynthetic products are released as soluble EPS (sEPS),[10] which are mainly composed of polysaccharides, proteins, lipids, nucleic acids, and other polymeric substances excreted by microorganisms.[11−13] EPS can interact with other charged particles via the functional groups in their macromolecules.[10,14−16] More so, the hydrophobic fractions of EPS polysaccharides can interact with other hydrophobic surfaces.[12] EPS derived from marine organisms were shown to affect the fate of carbon nanotubes,[14] copper nanoparticles,[15] modified nanoiron,[17] and ferrihydrite.[10] Similarly, studies have shown EPS can play a significant role in the toxicity of ENMs to both freshwater and marine organisms.[17−20] However, while EPS destabilized quantum-dots,[21] EPS improved the stability of carbon nanotubes.[14] Thus, the effect of sEPS on ENMs may be nanomaterial-chemical composition and coating specific, and needs further study.

The potential for sEPS to interact with coated $nTiO_2$, one of the most applied engineered nanomaterials, has not been investigated. Such interactions can lead to modification of ENM surface properties, which need to be accounted for when predicting the environmental implications of ENMs. The main

Received: July 25, 2016
Revised: October 16, 2016
Accepted: October 20, 2016
Published: October 21, 2016

DOI: 10.1021/acs.est.6b03684
Environ. Sci. Technol. 2016, 50, 12258−12265

objectives of this study were to (1) investigate the potential for interactions between three types of coated or uncoated commercial nTiO$_2$ and sEPS extracted from both freshwater and marine phytoplankton; (2) probe the effect of such interactions on the physicochemical properties and stability of the nanomaterials; and (3) conduct preliminary investigations on the mechanisms behind interactions between sEPS and coated nTiO$_2$.

2.0. MATERIALS AND METHODS

2.1. Engineered TiO$_2$ Nanoparticles. Hombikat UV 100 (denoted UV100), UV-Titan M212 (denoted M212), and UV Titan M262 (denoted M262) were obtained as dry ENM powders from Sachtleben, Germany, and used as received. According to the manufacturer, UV100 is uncoated, M212 has a hydrophilic alumina and glycerol coating, and M262 has a hydrophobic alumina and dimethicone polymer coating. The particle were thoroughly characterized and detailed information is given in Supporting Information (SI) section S1.0.

2.2. Extracellular Polymeric Substances (EPS). Soluble extracellular polymeric substances (sEPS) were extracted from axenic cultures of two algal species—*Chlamydomonas reinhardtii* (a freshwater phytoplankton) and *Dunaliella tertiolecta* (a seawater phytoplankton). *C. reinhardtii* was cultured in COMBO media while *D. tertiolecta* was cultured in f/2 media made with natural seawater collected from the Pacific Ocean (Santa Barbara, CA).[19,22] sEPS were extracted via centrifugation (2500g, 15 min, and 4 °C using a Sorvall RC 5B Plus centrifuge) when the cells reached stationary growth phase.[14] The supernatants, which contained sEPS, were aseptically filtered with 0.2 μm PES membrane filters (Thermo Fisher Scientific). To remove residual salts from the growth media and low molecular-weight metabolites, sEPS were dialyzed against DI water (renewed twice daily) for 5 d at 4 °C using a 3.5 kDa cutoff regenerated cellulose tubular membrane (Fisher Scientific). Completion of dialysis was confirmed by noting that the conductivity of dialysis media (DI water) remained stable after 2 d (freshwater) or 3 d (seawater) after media renewal. The dialysis membranes were treated with $NaHCO_3$ and Na_2EDTA to remove residues before use.

Dissolved organic carbon (DOC) and total dissolved nitrogen (TDN) of sEPS were measured using a Shimadzu TOC-V with a TNM1 unit. In addition, carbohydrate and protein concentrations were determined using the anthrone method[23] (with glucose as standard), and modified Lowry Protein Assay[24] (with bovine serum albumin as standard), respectively. ζ potential of sEPS (2 mg-C/L) at pH from 4 to 11 (adjusted with 0.5 mM buffers) was determined using the Zetasizer. Each zeta potential value was an average of three replicate measurements and each measurement consisted of 10−14 runs. Infrared spectroscopy of lyophilized sEPS was studied using a Nicolet iS10 spectrometer with a diamond ATR crystal. Interferograms were collected by taking 256 scans in the range 4000−400 cm^{-1} at 2 cm^{-1}.

2.3. GC-TOF-MS Analysis of EPS. The lyophilized sEPS were further characterized via gas chromatography time-of-flight mass spectrometry (GC-TOF-MS) at the West Coast Metabolomics Center (University of California Davis), to identify their constituent compounds. Details of extraction, instrumentation, and analytical methods were previously reported by Fiehn et al.[25] GC-TOF-MS analysis was also done on Suwannee River natural organic matter (SRNOM, obtained from International Humic Substances Society), a commonly used stabilizer in ENMs studies, for comparison.

2.4. Effect of sEPS on Surface Charge of nTiO$_2$. The effect of sEPS on the surface charge of nTiO$_2$ was determined by measuring the ζ potential of the particles (50 mg/L) in DI water with or without 0.5 mM carbonate buffer (pH 7) in the presence of sEPS (0−0.5 mg-C/L). The influence of carbonate buffer on ζ potential of the particles was also determined in order to clearly assess the contribution of sEPS to changes in the physicochemical properties of the nanoparticles. The effect of sEPS on the ζ potential of particles was compared to that of SRNOM (0.25 mg-C/L), which is a commonly used proxy for NOM. SRNOM was studied to determine how the influence of SRNOM on nTiO$_2$ surface charge and stability may be different from that of sEPS.

2.5. Effect of sEPS on Aggregation of nTiO$_2$. The effects of sEPS (0−0.5 mg-C/L) on the aggregation kinetics of UV100, M212, and M262 were studied via dynamic light scattering (DLS) as described previously[14,26] and explained in the SI section S2.0. Additional aggregation kinetics studies were conducted in the presence of 0.25 mg-C/L SRNOM for comparison.

2.5.1. Role of sEPS Type and Concentration. The composition of EPS varies widely with cell type, cell growth stage, nature of habitat, etc.[11−13] To investigate if the source of sEPS influenced its effect on nTiO$_2$ aggregation dynamics, we compared the effects of sEPS isolated from *C. reinhardtii* and *D. tertiolecta*. Separate nTiO$_2$ suspensions were made with 0.5−2 mg-C/L of sEPS from each organism. Similarly, the concentrations of EPS in natural waters is expected to vary temporally and spatially based on water productivity and nutrient availability, among other factors. To study the role of sEPS concentration, we prepared nTiO$_2$ stocks as described earlier with 0.5 to 2 mg-C/L of *C. reinhardtii* sEPS. All the analyses were done at pH 7 and final concentration of sEPS in the samples measured was 0, 0.125, 0.25, and 0.5 mg-C/L, respectively.

2.5.2. Role of Algal Media Nutrient Level. To see how variation in algal nutrient level may affect sEPS composition and its influence on nTiO$_2$ aggregation, we cultured *D. tertiolecta* in f/2 media with (1) normal nutrient levels and (2) with spiked nitrogen (twice the normal level or 17.64 × 10^{-4} M $NaNO_3$). Aggregation kinetics were compared using nTiO$_2$ stocks made with 1 mg-C/L of sEPS isolated from both sets of organisms. sEPS isolated from *C. reinhardtii* is hereafter referred to as sEPS-Chl. sEPS isolated from *D. tertiolecta* grown in normal f/2 media and f/2 media with spiked N are hereafter denoted as sEPS-Dun1 and sEPS-Dun2, respectively.

2.6. Interaction of sEPS with nTiO$_2$. UV100 was selected as a representative for the nTiO$_2$ and was used for further analysis investigating sEPS interactions with nTiO$_2$: To confirm the adsorption of sEPS unto nTiO$_2$, and to investigate the sEPS groups that are responsible for interactions with nTiO$_2$, we added 5 mg of UV100 to DI or sEPS stock solutions. The suspensions were sonicated for 1 h (Branson 2510) to allow for interactions after which they were centrifuged (12,000 g, 30 min). The aqueous phase (containing sEPS that were not adsorbed to nTiO$_2$) was decanted. The solid fractions obtained were lyophilized and then analyzed using the Nicolet FTIR spectrometer in absorbance mode (256 scans in the range 4000−400 cm^{-1} at a resolution of 2 cm^{-1}). Spectra from DI-suspended solids were subtracted from spectra from samples suspended in sEPS in order to remove signals due to nTiO$_2$.

DOI: 10.1021/acs.est.6b03684
Environ. Sci. Technol. 2016, 50, 12258−12265

The spectra obtained after the subtraction were then compared with spectra from lyophilized pristine sEPS stocks.

3.0. RESULTS AND DISCUSSION

3.1. nTiO$_2$ and sEPS Characterizations. TEM analyses showed that the primary particles of UV100 are about an order of magnitude smaller than those of M212 and M262 (Figure 1

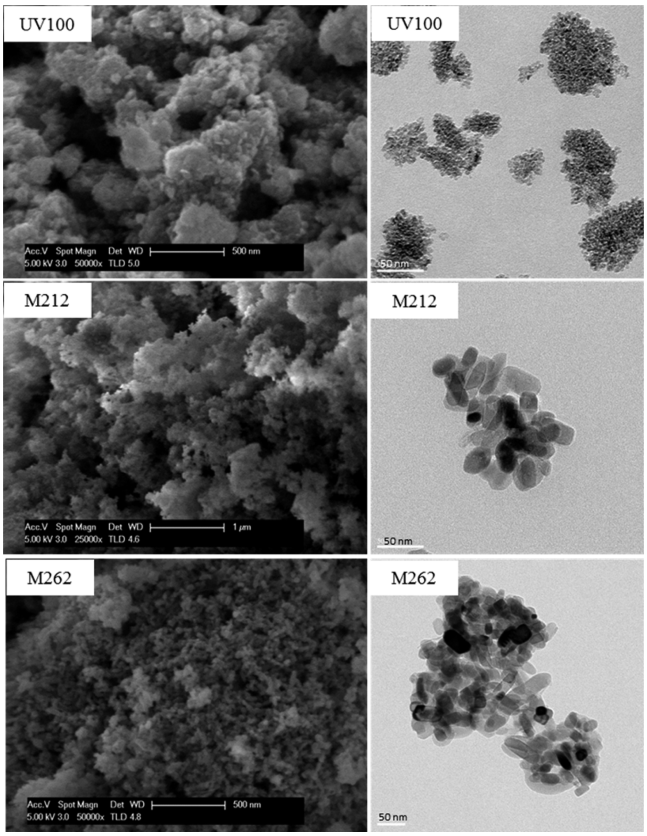

Figure 1. Scanning (left) and transmission (right) electron micrographs of UV100, M212, and M262 nTiO$_2$.

Table 1. Major Physicochemical Properties of TiO$_2$ Nanoparticles Used in This Study

property	UV100	M212	M262
average primary particle size (nm)	3.6	23	24
hydrodynamic diameter, HDD (nm)[a]	526	212	257
zeta potential (mV)[a]	3.3	31.9	32.4
isoelectric point (pH)	6.2	9.3	9.2
phase	anatase	rutile	rutile
crystal structure	tetragonal	tetragonal	tetragonal
BET surface area (m^2/g)	320	56.2	47.7

[a]Measurements were taken in DI (pH 5.8).

and SI Figure S1, Table 1). This is in agreement with BET data (Table 1). Sizes were determined from the average of 30−60 particles; particle size distributions are presented in SI Figure S2. EDS analyses (SI Figure S3) showed that UV100 was only composed of titanium (Ti) and oxygen (O). EDS revealed the presence of aluminum (Al, < 4% wt.) in M212 and M262, whereas M262 also contained silicon (Si, ∼ 1% wt.). Al 2p and Al 2s peaks were also observed in the XPS surveys of M212 and M262 at binding energy (BE) ≈ 74 and 118.5 eV, respectively (SI Figure S4). The presence of Si (siloxane bonds) on the surface of M262 was also confirmed via XPS as shown by the Si 2p$_{3/2}$ peak at BE ≈ 102.5 eV. These findings agree with the manufacturer's information regarding the coatings on M212 and M262, and further results of X-ray analyses were provided in SI section 3.0, and SI Figures S5−S6.

Despite its small primary particle size, UV100 formed the largest aggregates in water, with HDD more than twice that of M212 and M262 (Table 1). The instability of UV100 is probably due to its low surface charge in suspension as indicated by a ζ potential of 3.3 mV in DI. The ζ potential of M212 and M262 exceeded 30 mV, above the typical colloidal stability threshold.[27] The suspensions of the three nTiO$_2$ had pH = 5.8 in DI, which is below their respective IEPs (Table 1, Figure S7).

GC-TOF-MS results are presented in section S4.0; relative abundance of the most abundant compounds is presented in SI Figure S8. Table 2 shows the major properties of the three

Table 2. Major Characteristics of Soluble EPS Used in This Study

property	sEPS-Chl	sEPS-Dun1	sEPS-Dun2
dissolved organic carbon (mg-C/L)	8.46	14.3	16.9
total dissolved nitrogen (mg/L)	2.59	0.81	1.39
carbohydrate (mg/L-glucose equiv)	15.8	11.6	15.6
protein (mg/L-BSA equiv)	20.3	1.91	6.62
zeta potential in DI water (mV)	−12.7	−25.2	−22.1

sEPS used in this study. The three sEPS had net negative charges in DI and buffered solutions (Table 2, SI Figure S9). However, sEPS from *D. tertiolecta* was more negatively charged (p < 0.05), and more sensitive to pH than sEPS from *C. reinhardtii* (see caption of SI Figure S9). Increasing negative charge of sEPS with pH is typically due to deprotonation of carboxyl (pH 2.0−6.0), phospholipids (pH 2.4−7.2), phosphodiester (pH 3.2−3.5), amine (pH 9.0−11.0), and hydroxyl (pH ≥ 10) groups[28−30] present in their constituting metabolites. Although polysaccharides are generally considered the major EPS fraction, we observed a carbohydrate:protein mass ratio ranging from 0.8 (in *C. reinhardtii*) to 6.1 (in *D. tertiolecta*).

FTIR spectra of the three sEPS (SI Figure S10) are quite similar since their composition is qualitatively similar (Table 2). Detailed band assignments of the spectra are shown in SI Table S1a-c. FTIR spectrum of SRNOM was presented in a previous study.[15]

3.2. Effect of sEPS on Surface Charge of nTiO$_2$. The adsorption of various materials (e.g., ions, biomolecules, polymers, colloids) onto the surface of ENMs often influences their surface charge, which influences their stability in different media. The presence of sEPS affected the ζ potential of the three nTiO$_2$ (Figure 2). Adding only carbonate buffer reduced the ζ potential of M262 from 32.4 to 21.6 mV, probably due to the attachment of carbonate ions on the particle surface. ζ potential of M262 was further reduced to −2.99, −10.7, and −11.5 in the presence of 0.125, 0.25, and 0.5 mg-C/L sEPS-Chl, respectively. The ζ potential of M262 at 0.25 and 0.5 mg-C/L suggest that the surface of M262 was coated with algal polymers whose ζ potential was measured at −12.7 mV (Table 2). Similar results were observed with sEPS-Dun1 and sEPS-

DOI: 10.1021/acs.est.6b03684
Environ. Sci. Technol. 2016, 50, 12258−12265

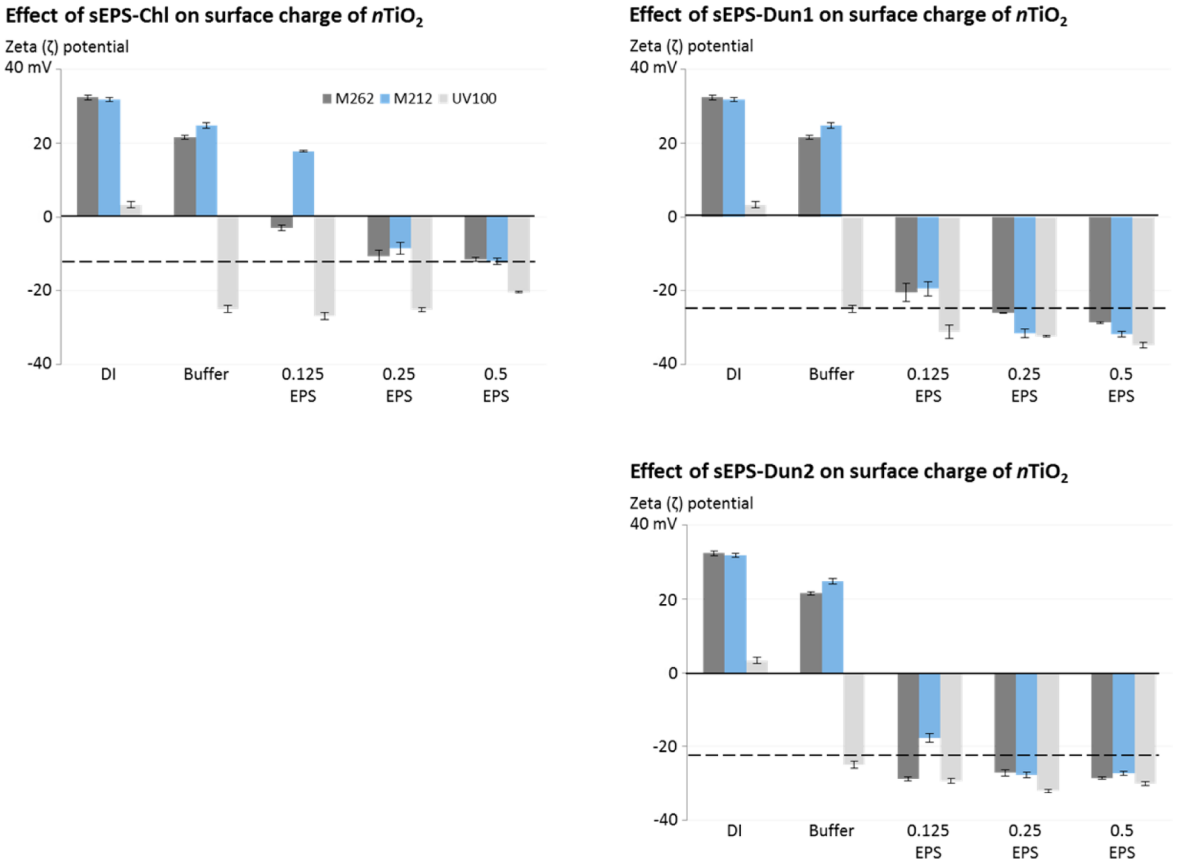

Figure 2. Effect of carbonate buffer (Buffer) and sEPS on the ζ potentials of nTiO$_2$. Broken horizontal lines represent the ζ potentials of sEPS. pH 7 except in DI (pH 5.8).

Dun2 when present in the stock of both M262 and M212, with the ζ potential of particles shifted toward that of the respective sEPS at increasing sEPS concentrations. At 0.25 mg-C/L of sEPS-Dun1 and sEPS-Dun2, ζ potential of the three nTiO$_2$ was essentially that of sEPS.

Since UV100 was already negatively charged (−25 mV) in the presence of buffer, the surface charge information cannot confirm that it is coated by sEPS. The addition of sEPS-Chl (up to 0.5 mg-C/L) only slightly increased ζ potential of UV100 to −23.7 mV. There is low electrostatic attraction between UV100 and sEPS, since both have net negative charges at pH 7. Although sEPS are negatively charged, they do contain some positively charged moieties (e.g., amino groups in proteins) that can interact electrostatically with the negatively charged UV100 surface.

In addition, UV100 has a much greater surface area (320 m^2/g) than M212 and M262 (~50 m^2/g for both) hence, much more sEPS would be needed to cover the surface of the UV100 compared to M212 and M262. At the highest concentration of sEPS used, the ratio of sEPS concentration per unit area of the surface of UV100 (1.56×10^{-3} mg-C.g/m^2.L) is about an order of magnitude less than that of a similar mass of M212 (0.89×10^{-2} mg-C.g/m^2.L) or M262 (1.05×10^{-2} mg-C.g/m^2.L).

Interactions between SRNOM (0.25 mg-C/L) and the three nTiO2 led to more negatively charged particle surfaces (SI Figure S11) than with sEPS. Thus, sEPS and other NOM can interact with both positively and negatively charged coated and uncoated nTiO$_2$ in aqueous media. However, they may coat positively (or neutrally) charged particles more effectively due to stronger electrostatic interactions. sEPS coating may lead to a reversal of surface charge as seen in M212 and M262 at sEPS concentrations that are environmentally relevant (up to 3.7 mg-C/L has been reported in the literature).[31] In addition, the strong influence of sEPS on the surface charge of the positively charged nTiO$_2$ suggests the formation of anionic negatively charged surface complexes. Like most charged surfaces, ionic strength and pH can affect the surface charge of sEPS,[28] which can affect the strength of their attractive interactions with nTiO$_2$.

3.3. Effect of sEPS on Aggregation of nTiO$_2$. ENM stability in aquatic systems can be reasonably predicted from their critical coagulation concentration (CCC). The CCC of all three nTiO$_2$ in the presence of NaCl decreased as pH approached their respective IEPs (Figure 3). Although M212 and M262 are essentially the same core particle, M262 was much less stable in aqueous media across the range of pH studied. This is probably due to surface hydrophobicity of its coating. Of the three nTiO$_2$, M212 was the most stable in acidic conditions while UV100 was the most stable in alkaline conditions. This finding clearly shows that predictions of the environmental fate of ENMs cannot be adequately made just using their chemical composition, size, or even surface charge.

In general, sEPS-Chl influenced the CCC of the three nTiO$_2$. The CCC of all nTiO$_2$ increased with increasing amounts of sEPS (Figure 4a). For instance, the CCC of M262 at pH 7 increased by an order of magnitude from 5.5 mM NaCl in the absence of sEPS-Chl to 63 mM NaCl in the presence of 0.5 mg-C/L sEPS-Chl. Typical ionic strength of freshwater systems is 5−10 mM, which implies that pristine M262 will be quite unstable in natural waters and exposure to pelagic organisms

DOI: 10.1021/acs.est.6b03684
Environ. Sci. Technol. 2016, 50, 12258−12265

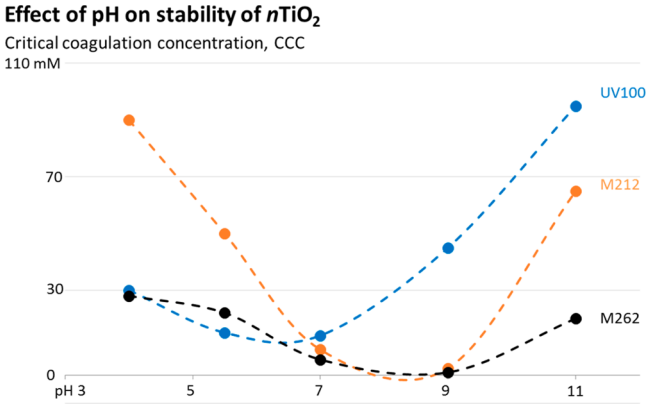

Figure 3. Critical coagulation concentrations, CCC (in mM NaCl) of nTiO$_2$ as a function of pH. RSD for repeated experiments was <10%.

(e.g., algae) would be low. The adsorption of algal sEPS on M262 however will increase the stability of the nTiO$_2$ in aqueous media, which may lead to an increase in the exposure of pelagic organisms to an otherwise relatively unstable ENM. Increased stability of the nTiO$_2$ by sEPS is due to steric hindrance between particle aggregates imparted by the algal macromolecules. Since UV100 is much smaller and more spherical than M212 and M262 (which are mostly cubic and elongated as shown in SI Figure S1), UV100 has a much larger radius of curvature than the coated particles. This implies that sEPS macromolecules will experience decreasing steric hindrance among themselves as one moves away from the nTiO$_2$ surface and much more sEPS can potentially adsorb onto the surface of UV100 than M212 and M262. In addition to steric stabilization, the charged groups on EPS can also impart some electrostatic stabilization on the ENMs they adsorb onto as we reported in the previous section and other studies.[14,15,17]

The effect on stability of nTiO$_2$ by sEPS-Dun1, extracted from a marine phytoplankton, compared reasonably well with that of sEPS-Chl, which was extracted from a freshwater phytoplankton (Figure 4b). However, stronger influence on stability (i.e., increased CCC) of all three ENMs was observed in the presence of sEPS-Dun2, isolated from D. *tertiolecta* that was cultured in N-spiked media. The mechanism behind the higher stabilizing potential of sEPS-Dun2 is not very clear: Although sEPS-Dun2 had a higher DOC than sEPS-Dun1 and sEPS-Chl (Table 2) this may not account for increased stability since the DOC of all three types of sEPS was normalized for the entire study. Similarly, there is no correlation between the observed effects on CCC and the abundance of any of the sEPS metabolites. Further studies, using a much larger number of different sEPS types, need to be conducted to decipher how the specific composition of sEPS influences their ENM-stabilizing properties. The relationships between sEPS properties such as molecular weight, functional group density, and configuration characteristics, etc. and their interactions with ENMs also need further study.

At low concentrations of sEPS and SRNOM (0.125 and 0.25 mg-C/L) we found a negative correlation between the ratio of DOC/nanoparticle surface area and CCC (with R^2 value >0.99 for sEPS and >0.97 for SRNOM; SI Figure S12). That is, at similar sEPS/SRNOM and nanoparticle concentrations, the CCC determined for UV100 was much higher than the CCC determined for M262 and M212 despite UV100 having as much as 5−6 times less DOC per unit of its surface area. This is quite counterintuitive as one would expect higher nanoparticle stability at higher NOM concentrations due to improved electrosteric stabilization. This finding suggests that the surface properties (area and modified charge) of each nTiO$_2$ played an important role in their interactions with the sEPS macromolecules (e.g., surface charge can determine the conformation of the macromolecules on the surface of the nanoparticles).

The conformation of sEPS macromolecules attached to all the nTiO$_2$ particles is expected to differ based on the charge, surface area, and perhaps hydrophobicity of the surfaces of the ENMs. At pH 7 for instance (where M212 and M262 are positively charged, and UV100 is negatively charged; Figure S7), one would expect sEPS to be less tightly bound to UV100 than to M212 and M262 (as explained earlier in section 3.2). Particles with looser EPS binding/conformation may experience fewer successful collisions since a relatively larger fraction of sEPS polymers is free to exert steric effects than in particles where sEPS is tightly bound (SI Scheme S1). However, at higher sEPS concentrations (e.g., 0.5 mg-C/L as in this study or higher) particles with tightly bound sEPS may experience higher stability since more successful collisions may not

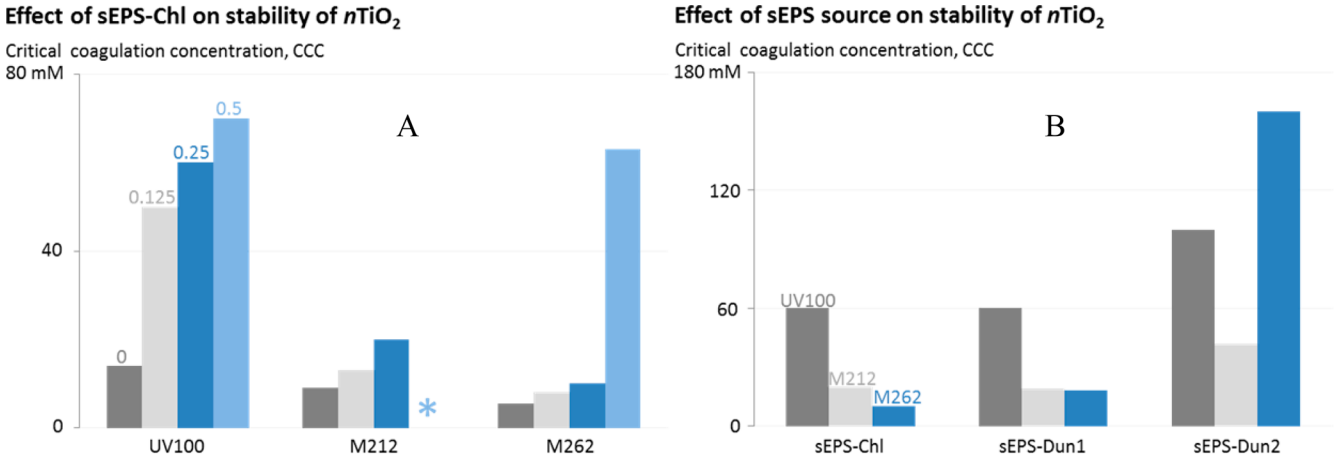

Figure 4. (A) Effect of sEPS-Chl (0.125−0.5 mg-C/L) on CCC (mM NaCl) of nTiO$_2$ in NaCl at pH 7. *M212 was stable in the presence of 0.5 mg-C/L sEPS-Chl (up to 800 mM NaCl); hence CCC could not be determined. (B) Comparison of CCC of nTiO$_2$ in the presence of 0.25 mg-C/L sEPS-Chl, sEPS-Dun1, and sEPS-Dun2 at pH 7. RSD for repeated experiments was <10%.

DOI: 10.1021/acs.est.6b03684
Environ. Sci. Technol. 2016, 50, 12258−12265

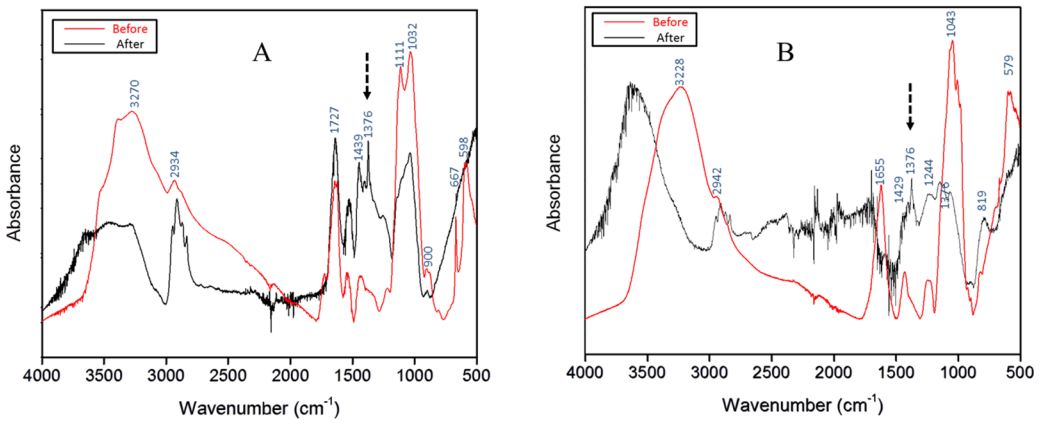

Figure 5. FTIR spectra of sEPS isolated from (A) *C. reinhardtii* and (B) *D. tertiolecta* before and after interactions with UV100 nTiO$_2$ (The noise in the spectra after interactions is due to the low (yet environmentally relevant) concentrations of sEPS).

necessarily result in increased attachment (since their surface will be completely covered). This may explain why sEPS appeared to have more stabilizing effects on UV100 than M262 and M212 (despite both coated nTiO$_2$ types having a much higher sEPS density on tier surfaces than UV100 with higher surface area), except at the highest concentration of sEPS-Chl (Figure 4a).

A comparison of the effect of different concentrations (0.125−0.5 mg-C/L) of sEPS-Chl and SRNOM on the CCC of the three nTiO$_2$ is presented in SI Table S2. Clearly, the stabilizing effect of sEPS compares well with that of SRNOM, which is commonly used as a stabilizer for ENMs in aqueous media. The data also showed a stronger stabilizing effect of sEPS (than SRNOM) at 0.5 mg-C/L, especially for the coated rutile phase nTiO$_2$ (M212 and M262). Although the raw materials for making SRNOM and other similar NOM proxies are originally obtained from the natural environment, the NOM proxies are products of several physical and chemical processes conducted by the suppliers to purify and preserve them. Some of these processes may change the physicochemical properties of the NOM molecules such that they no longer reflect the true nature of organic materials in real aquatic systems.[32] As such, sEPS (obtained from natural sources such as bacteria, algae, etc. without further processing), which are also able to provide similar or superior ENM stabilizing effects, may be better surrogates for naturally occurring organic matter in laboratory investigations.

3.4. Mechanism of nTiO$_2$-sEPS Interactions. We compared the FTIR spectra of pristine sEPS to those collected after allowing the biopolymers to interact with nTiO$_2$ in order to identify the functional groups that are responsible for interactions with the ENMs (Figure 5). Adsorption of sEPS onto nTiO$_2$ modified the spectra of the macromolecules. In Figure 5a for instance, the bands around 3270 and 3387 cm^{-1}, (symmetric and asymmetric stretch of NH$_2$ in primary amides, respectively) decreased in intensity and shifted to higher wavenumbers after sEPS interacted with nTiO$_2$. Similarly, the C═O out-of-plane band in amides at around 598 cm^{-1} disappeared. The bands around 1439 and 1220 cm^{-1} (OH bending in carboxylic acids and P═O stretching of phospholipids or nucleic acids, respectively) shifted to 1450 and 1260 cm^{-1}, respectively. The band for O−C═O bending in carboxylic acid around 667 cm^{-1} disappeared. Band shifts and disappearance after interactions indicate the functional groups that are involved in adsorption/complexation.[29,33,34] A new band emerged around 1376 cm^{-1} which is consistent with the symmetric stretch of COO$^-$ group in carboxylic acid salts,[35] suggesting the formation of a chemical bond between the carboxylic group and the surface of nTiO$_2$.[33,36] The corresponding asymmetric stretch of COO$^-$ band was probably masked by the carboxylic acid OH bending band around 1460 cm^{-1}. Bonds between COO$^-$ group and nTiO$_2$ are typically formed via bridge-coordination, which may involve the binding of one or both oxygens of the deprotonated carboxylic acid to surface titanium ions.[33,36,37]

Interactions between sEPS and nTiO$_2$ occurred via amide, hydroxyl, and carboxylic groups of sEPS amino acids, as well as phosphate groups in phospholipids or nucleic acids. Emergence of a new COO$^-$ band and the disappearance of an O−C═O group are consistent with inner sphere complexation of sEPS on nTiO$_2$.[29,36] Our findings agree to some extent with other studies that have probed the interactions between metallic oxides and microbial macromolecules. For instance, Fang et al. found that bacterial EPS proteins adsorbed onto goethite but phosphate groups were responsible for the formation of chemical bonds.[29] Proteinaceous components of EPS were also involved in the adsorption of the biopolymer to montmorillonite and kaolinite.[38]

Although the strength of adsorption of sEPS on nTiO$_2$ via electrostatic interactions depends on media chemistry such as pH and ionic strength, the existence of chemical bonding between sEPS macromolecules and nTiO$_2$ will make the association strong and possibly long-lived. As a result, the modification of the surface properties of nTiO$_2$ brought about by associated sEPS may persist (although sEPS may be liable to biodegradation or catalytic degradation from nTiO$_2$). More so, these surface-modified nTiO$_2$ (and possibly other metallic ENMs) are probably the form that aquatic organisms will be exposed to in the long term and an understanding of their effects—as different from those of pristine ENMs—is imperative for ENM risk assessment.

4.0. ENVIRONMENTAL IMPLICATIONS

In natural waters, ENMs will interact with other biogenic and geogenic matter that are present, including sEPS. These interactions may lead to physisorption and/or chemisorption of sEPS on the surface of the ENMs, which may change the physicochemical properties and fate of the particles. sEPS may lead to charge reversal of positively charged nTiO$_2$ ENMs, which will play an important role in the bioavailability of ENMs

DOI: 10.1021/acs.est.6b03684
Environ. Sci. Technol. 2016, 50, 12258−12265

to organisms, their interactions with other charged surfaces (e.g., membranes of bacteria), and their overall effect on biota.

Chemisorption of sEPS to nTiO$_2$ implies that the biomacromolecules may not be easily desorbed from the ENMs. As a result, the effects of sEPS on nTiO$_2$ properties, fate, and effects in natural waters may not be short-lived. Degradation of sEPS or their utilization as nutrient sources by heterotrophs may however interfere with the sEPS-ENM association. For instance, the catalytic properties of ENMs such as nTiO$_2$ can degrade biopolymers such as sEPS, similar to their effect on cellular membranes.[39] sEPS are also used by heterotrophs as carbon source, although it is possible that the bioavailability of sEPS associated with nTiO$_2$ will be somewhat different.

Surface coating of ENMs clearly plays an important role in their stability, fate and exposure. In this study for instance, the poor stability of M262 in aqueous media (compared to M212 which has a similar core) due to its hydrophobic surface coating implies that pelagic organisms will be less exposed to M262 relative to M212 when released into water (e.g., from the matrix of sunscreens). Attachment of sEPS onto the surface of ENMs with low stability (like M262) may however improve their stability in water such that the fate and effects of the ENMs cannot be simply predicted based on the intrinsic physicochemical properties of the particles.

■ ASSOCIATED CONTENT

Supporting Information

The Supporting Information is available free of charge on the ACS Publications website at DOI: 10.1021/acs.est.6b03684.

Section S1.0 showing aggregation kinetics method. Figure S1−S9 showing characterizations of nTiO2 and sEPS. Table S1−S3 showing major characteristics and FTIR band assignment of sEPS; and comparison of the effect of sEPS and SRNOM on stability of nTiO$_2$. Scheme S1 showing the effect of ENM surface charge on the conformation of adsorbed sEPS (PDF)

■ AUTHOR INFORMATION

Corresponding Authors

*Phone: (+1)401-782-3065; e-mail: adeleye.adeyemi@epa.gov.
*Phone: (+1)805-893-7548; fax: (+1)805-893-7612; e-mail: keller@bren.ucsb.edu.

Present Address

†(A.S.A.) National Research Council Research Associate, Atlantic Ecology Division, US Environmental Protection Agency, Narragansett, Rhode Island, United States.

Notes

The authors declare no competing financial interest.

■ ACKNOWLEDGMENTS

This material is based upon work supported by the NSF and the EPA under Cooperative Agreement Number DBI 0830117. Any opinions, findings, and conclusions or recommendations expressed in this material are those of the authors and do not necessarily reflect the views of NSF or EPA. We thank the MRL Central Facilities, which are supported by the MRSEC Program of the NSF under Award No. DMR 1121053, for the use of their instruments. We also thank Paige Rutten for lab assistance, and Dr. Louise Stevenson for providing *C. reinhardtii* cultures.

■ REFERENCES

(1) Keller, A. A.; McFerran, S.; Lazareva, A.; Suh, S. Global life cycle releases of engineered nanomaterials. *J. Nanopart. Res.* **2013**, *15* (6), 1−17.

(2) Gondikas, A. P.; Kammer, F. v. d.; Reed, R. B.; Wagner, S.; Ranville, J. F.; Hofmann, T. Release of TiO2 Nanoparticles from Sunscreens into Surface Waters: A One-Year Survey at the Old Danube Recreational Lake. *Environ. Sci. Technol.* **2014**, *48* (10), 5415−5422.

(3) Keller, A. A.; Wang, H.; Zhou, D.; Lenihan, H. S.; Cherr, G.; Cardinale, B. J.; Miller, R.; Ji, Z. Stability and Aggregation of Metal Oxide Nanoparticles in Natural Aqueous Matrices. *Environ. Sci. Technol.* **2010**, *44* (6), 1962−1967.

(4) Thio, B. J. R.; Zhou, D.; Keller, A. A. Influence of natural organic matter on the aggregation and deposition of titanium dioxide nanoparticles. *J. Hazard. Mater.* **2011**, *189* (1−2), 556−563.

(5) Zhou, D.; Ji, Z.; Jiang, X.; Dunphy, D. R.; Brinker, J.; Keller, A. A. Influence of material properties on TiO2 nanoparticle agglomeration. *PLoS One* **2013**, *8* (11), e81239.

(6) Wang, H.; Adeleye, A. S.; Huang, Y.; Li, F.; Keller, A. A. Heteroaggregation of nanoparticles with biocolloids and geocolloids. *Adv. Colloid Interface Sci.* **2015**, *226* (Pt A), 24−36.

(7) Praetorius, A.; Labille, J.; Scheringer, M.; Thill, A.; Hungerbühler, K.; Bottero, J.-Y. Heteroaggregation of Titanium Dioxide Nanoparticles with Model Natural Colloids under Environmentally Relevant Conditions. *Environ. Sci. Technol.* **2014**, *48* (18), 10690−10698.

(8) Quik, J. T. K.; Velzeboer, I.; Wouterse, M.; Koelmans, A. A.; van de Meent, D. Heteroaggregation and sedimentation rates for nanomaterials in natural waters. *Water Res.* **2014**, *48*, 269−279.

(9) Erhayem, M.; Sohn, M. Stability studies for titanium dioxide nanoparticles upon adsorption of Suwannee River humic and fulvic acids and natural organic matter. *Sci. Total Environ.* **2014**, *468−469* (0), 249−257.

(10) Kadar, E.; Cunliffe, M.; Fisher, A.; Stolpe, B.; Lead, J.; Shi, Z. Chemical interaction of atmospheric mineral dust-derived nanoparticles with natural seawater — EPS and sunlight-mediated changes. *Sci. Total Environ.* **2014**, *468−469* (0), 265−271.

(11) Wingender, J.; Neu, T.; Flemming, H., Microbial Extracellular Polymeric Substances: Characterisation. In *Structure and Function*; Springer, Berlin, 1999, 123.

(12) Flemming, H.-C.; Neu, T. R.; Wozniak, D. J. The EPS matrix: the "house of biofilm cells. *J. Bacteriol.* **2007**, *189* (22), 7945−7947.

(13) Underwood, G. J.; Boulcott, M.; Raines, C. A.; Waldron, K. Environmental Effects on Exopolymer Production by Marine Benthic Diatoms: Dynamics, Changes in composition, and Pathways of Production1. *J. Phycol.* **2004**, *40* (2), 293−304.

(14) Adeleye, A. S.; Keller, A. A. Long-term colloidal stability and metal leaching of single wall carbon nanotubes: effect of temperature and extracellular polymeric substances. *Water Res.* **2014**, *49* (0), 236−50.

(15) Adeleye, A. S.; Conway, J. R.; Perez, T.; Rutten, P.; Keller, A. A. Influence of Extracellular Polymeric Substances on the Long-Term Fate, Dissolution, and Speciation of Copper-Based Nanoparticles. *Environ. Sci. Technol.* **2014**, *48* (21), 12561−12568.

(16) Pal, A.; Paul, A. Microbial extracellular polymeric substances: central elements in heavy metal bioremediation. *Indian J. Microbiol.* **2008**, *48* (1), 49−64.

(17) Adeleye, A. S.; Stevenson, L. M.; Su, Y.; Nisbet, R. M.; Zhang, Y.; Keller, A. A. Influence of Phytoplankton on Fate and Effects of Modified Zerovalent Iron Nanoparticles. *Environ. Sci. Technol.* **2016**, *50* (11), 5597−605.

(18) Miao, A.-J.; Schwehr, K. A.; Xu, C.; Zhang, S.-J.; Luo, Z.; Quigg, A.; Santschi, P. H. The algal toxicity of silver engineered nanoparticles and detoxification by exopolymeric substances. *Environ. Pollut.* **2009**, *157* (11), 3034−3041.

(19) Stevenson, L. M.; Dickson, H.; Klanjscek, T.; Keller, A. A.; McCauley, E.; Nisbet, R. M. Environmental feedbacks and engineered nanoparticles: mitigation of silver nanoparticle toxicity to Chlamydo-

DOI: 10.1021/acs.est.6b03684
Environ. Sci. Technol. 2016, 50, 12258−12265

monas reinhardtii by algal-produced organic compounds. *PLoS One* **2013**, *8* (9), e74456.
(20) Zhang, S.; Jiang, Y.; Chen, C.-S.; Creeley, D.; Schwehr, K. A.; Quigg, A.; Chin, W.-C.; Santschi, P. H. Ameliorating effects of extracellular polymeric substances excreted by Thalassiosira pseudonana on algal toxicity of CdSe quantum dots. *Aquat. Toxicol.* **2013**, *126* (0), 214−223.
(21) Zhang, S.; Jiang, Y.; Chen, C.-S.; Spurgin, J.; Schwehr, K. A.; Quigg, A.; Chin, W.-C.; Santschi, P. H. Aggregation, dissolution, and stability of quantum dots in marine environments: Importance of extracellular polymeric substances. *Environ. Sci. Technol.* **2012**, *46* (16), 8764−8772.
(22) Miller, R. J.; Bennett, S.; Keller, A. A.; Pease, S.; Lenihan, H. S. TiO_2 Nanoparticles Are Phototoxic to Marine Phytoplankton. *PLoS One* **2012**, *7* (1), e30321.
(23) Morris, D. L. Quantitative Determination of Carbohydrates with Dreywoods Anthrone Reagent. *Science* **1948**, *107* (2775), 254−255.
(24) Legler, G.; Mullerplatz, C. M.; Mentgeshettkamp, M.; Pflieger, G.; Julich, E. On the Chemical Basis of the Lowry Protein Determination. *Anal. Biochem.* **1985**, *150* (2), 278−287.
(25) Fiehn, O.; Wohlgemuth, G.; Scholz, M.; Kind, T.; Lee, D. Y.; Lu, Y.; Moon, S.; Nikolau, B. Quality control for plant metabolomics: reporting MSI-compliant studies. *Plant J.* **2008**, *53* (4), 691−704.
(26) Saleh, N. B.; Pfefferle, L. D.; Elimelech, M. Aggregation Kinetics of Multiwalled Carbon Nanotubes in Aquatic Systems: Measurements and Environmental Implications. *Environ. Sci. Technol.* **2008**, *42* (21), 7963−7969.
(27) Everett, D. Basic principles of colloid science. *Royal Society of Chemistry paperbacks* **1988**, P001.
(28) Martinez, R. E.; Smith, D. S.; Kulczycki, E.; Ferris, F. G. Determination of Intrinsic Bacterial Surface Acidity Constants using a Donnan Shell Model and a Continuous pKa Distribution Method. *J. Colloid Interface Sci.* **2002**, *253* (1), 130−139.
(29) Fang, L.; Cao, Y.; Huang, Q.; Walker, S. L.; Cai, P. Reactions between bacterial exopolymers and goethite: A combined macroscopic and spectroscopic investigation. *Water Res.* **2012**, *46* (17), 5613−5620.
(30) Jiang, W.; Saxena, A.; Song, B.; Ward, B. B.; Beveridge, T. J.; Myneni, S. C. B. Elucidation of Functional Groups on Gram-Positive and Gram-Negative Bacterial Surfaces Using Infrared Spectroscopy. *Langmuir* **2004**, *20* (26), 11433−11442.
(31) Hung, C. C.; Tang, D. G.; Warnken, K. W.; Santschi, P. H. Distributions of carbohydrates, including uronic acids, in estuarine waters of Galveston Bay. *Mar. Chem.* **2001**, *73* (3−4), 305−318.
(32) Grasso, D.; Chin, Y.-P.; Weber, W. J. Structural and behavioral characteristics of a commercial humic acid and natural dissolved aquatic organic matter. *Chemosphere* **1990**, *21* (10), 1181−1197.
(33) Ojamäe, L.; Aulin, C.; Pedersen, H.; Käll, P.-O. IR and quantum-chemical studies of carboxylic acid and glycine adsorption on rutile TiO2 nanoparticles. *J. Colloid Interface Sci.* **2006**, *296* (1), 71−78.
(34) Bouhekka, A.; Bürgi, T. In situ ATR-IR spectroscopy study of adsorbed protein: Visible light denaturation of bovine serum albumin on TiO2. *Appl. Surf. Sci.* **2012**, *261* (0), 369−374.
(35) Lambert, J. B.; Shurvell, H. F.; Lightner, D. A.; Cooks, R. G. *Introduction to Organic Spectroscopy*; Macmillan: New York, 1987.
(36) Parikh, S. J.; Kubicki, J. D.; Jonsson, C. M.; Jonsson, C. L.; Hazen, R. M.; Sverjensky, D. A.; Sparks, D. L. Evaluating Glutamate and Aspartate Binding Mechanisms to Rutile (α-TiO2) via ATR-FTIR Spectroscopy and Quantum Chemical Calculations. *Langmuir* **2011**, *27* (5), 1778−1787.
(37) Zhang, G.; Kim, G.; Choi, W. Visible light driven photocatalysis mediated via ligand-to-metal charge transfer (LMCT): an alternative approach to solar activation of titania. *Energy Environ. Sci.* **2014**, *7* (3), 954−966.
(38) Cao, Y.; Wei, X.; Cai, P.; Huang, Q.; Rong, X.; Liang, W. Preferential adsorption of extracellular polymeric substances from bacteria on clay minerals and iron oxide. *Colloids Surf., B* **2011**, *83* (1), 122−127.
(39) Kiwi, J.; Nadtochenko, V. Evidence for the Mechanism of Photocatalytic Degradation of the Bacterial Wall Membrane at the TiO2 Interface by ATR-FTIR and Laser Kinetic Spectroscopy. *Langmuir* **2005**, *21* (10), 4631−4641.

DOI: 10.1021/acs.est.6b03684
Environ. Sci. Technol. 2016, 50, 12258−12265